Eur. Phys. J. A (2024) 60:203
https://doi.org/10.1140/epja/s10050-024-01420-5

THE EUROPEAN PHYSICAL JOURNAL A

Regular Article - Experimental Physics

Measurement of cross section of proton-induced reactions on oxygen with silicon dioxide target

Joanna Matulewicz[1,3,a], **Izabela Skwira-Chalot**[1], **Sebastian Kusyk**[2], **Tomasz Matulewicz**[1], **Przemyslaw Sękowski**[1], **Adam Spyra**[1], **Jan Swakoń**[2], **Wiktoria Szcześniak**[1], **Agata Taranienko**[1], **Damian Wróbel**[2]

[1] Faculty of Physics, University of Warsaw, 02-093 Warsaw, Poland
[2] Institute of Nuclear Physics, Polish Academy of Sciences, 31-342 Kraków, Poland
[3] National Centre for Nuclear Research, 05-400 Otwock, Poland

Received: 13 June 2024 / Accepted: 16 September 2024

Communicated by Alessia Di Pietro

Abstract Oxygen is one of the most common elements in the human body. Proton beams used in therapy induce nuclear reactions that cause a loss of fluence along the beam path. These reactions often lead to production of β^+ emitters with relatively short half-lives (less than 20 min). Cross sections for reactions on oxygen are not sufficiently known, particularly at proton energies above few tens of MeV. This contribution presents the results of an experiment, where silicon dioxide targets were used to study nuclear reactions induced by protons with energy below 60 MeV on oxygen. The proton beam was delivered by the AIC-144 cyclotron of the Institute of Nuclear Physics in Kraków. Cross sections of reactions leading to production of ^{11}C, ^{13}N and ^{15}O were obtained. They agree well with the measurements using Cherenkov radiation in bulk SiO_2. The recent measurements performed with a PET scanner provided similar results, except in the case of ^{16}O(p,x)^{11}C reaction studied in the energy of up to 200 MeV, where our results are 30% lower.

1 Introduction

During proton therapy, protons can induce nuclear reactions that decrease the beam fluence and impact the dose distribution [1]. The secondary target fragments produced in the nuclear reactions contribute to the dose deposited also to the healthy tissues, which may increase the risk for secondary cancer [2]. This is especially significant in the entrance of the beam, contributing to an estimated 10% of the biological effect in this region [3]. Precise description of the impact of nuclear reactions requires experimental cross sections. One of the most common elements in human body is oxygen, making up 24% of the atoms. Cross-section of reactions induced by protons on oxygen was measured in numerous experiments performed during the past seven decades at beam energies from the reaction threshold up to the relativistic regime. The principal information about the applied method, targets, experimental set-up and beam energy is provided in the Appendix. The whole energy range used in proton therapy, which is up to 250 MeV, is not yet fully studied. The available experimental cross sections data on these reactions show some inconsistencies and the production cross sections of not all β^+ emitters (e.g ^{13}N) have been measured with the expected precision. Therefore, continuous experimental activities are needed to provide the necessary inputs to models describing the beam interaction with the tissue.

Four measurements performed in the past decade should be mentioned as relevant for the proton therapy physics:

- The measurements on the production of 3 isotopes (^{11}C, ^{13}N and ^{15}O) at 9 proton beam energies below 70 MeV, where the decay of β^+ emitters was studied with the PET device [4]. Significant discrepancies of the results with previous ones were observed particularly for the production of ^{13}N.
- Very detailed energy scan at energies below 70 MeV was performed for the mentioned 3 radionuclides with a novel method of measuring the Cherenkov radiation in bulk SiO_2 crystal read by CCD device [5]. These results have been normalized to the ^{15}O yield at 35 MeV (taken from the literature).
- Production of ^{11}C and ^{15}O was performed for proton energies below 220 MeV (8 and 5 experimental points, respectively) [6]. Experimental correction to the coincidence yield of two 511 keV photons has been provided by

[a] e-mail: jm.matulewicz@student.uw.edu.pl (corresponding author)

Published online: 09 October 2024

the third BaF_2 detector placed at 90° with respect to the two scintillators placed back-to back around the target.

- Extensive measurements of the production of ^{11}C, ^{13}N and ^{15}O at energies from 20 to 200 MeV [7] on carbon, AlN (aluminium nitride) and SiO_2 targets. At lower energies the β^+ activity was measured by a pair of $LaBr_3$ detectors, while at higher energies in a PET device.

The aim of the experiment was to measure the cross-section at proton energy range below 60 MeV, where the results can be compared to the existing data mentioned above. This comparison is important to evaluate the applicability of the method, which might be used in the future measurements at higher energies. The other purpose was to compare two methods of measurement: standard decay spectroscopy of irradiated target and sampled measurement of simultaneously irradiated numerous targets using a limited number of detector pairs registering β^+ activity. The measurements were performed with 15 and 3 simultaneously irradiated solid SiO_2 wafers of optical quality.

2 Experiment

Oxygen is a difficult target for nuclear physics experiments, as it is gaseous above 90 K (normal conditions). Therefore, a solid target made of silicon dioxide was chosen for this experiment. While the common products of proton reactions on oxygen decay within 2–20 min (see Table 1), proton-induced reactions on silicon produce mostly isotopes with very short half-lives (less than 10 s) [8] or very long half-lives (more than 1 year). The only activity that might be measured is the β^+ decay of ^{18}F with half-life 109.77(5) min [9]. However, ^{18}F is produced only in reactions on heavier isotopes ^{29}Si and ^{30}Si, which constitute less than 8% of natural silicon. Moreover, the predicted cross-section for production of ^{18}F is less than 1 mb for proton energies below 60 MeV [10]. For these reasons, only reactions on oxygen were taken into consideration.

A set of 15 silicon dioxide targets was manufactured in Pracownia Optyki Instrumentalnej in Józefów, Poland. The samples had a diameter of 10 mm, a thickness of approximately 0.9 mm and weight of 0.18 g.

Table 1 Reactions induced by protons on oxygen, their Q-values and half-lives of produced β^+ emitters [9]

Reaction	Q-value [MeV]	Residue	$T_{1/2}$ [min]
$^{16}O(p,d+\alpha)$	− 23.7	^{11}C	20.36 (2)
$^{16}O(p,\alpha)$	−5.2	^{13}N	9.965 (4)
$^{16}O(p,d)$	− 13.4	^{15}O	2.041 (6)

For each residue only reactions with the lowest Q-value are listed

The irradiation was carried out at the Institute of Nuclear Physics PAS in Kraków, Poland. During each measurement, chosen targets were stacked next to each other and irradiated with a proton beam delivered by AIC-144 cyclotron. Two irradiations were conducted, with beam energies 58 and 40 MeV. The details are listed in Table 2.

The detection setup (see Fig. 1) was designed and constructed at the Faculty of Physics of University of Warsaw [11]. It consists of six cylindrical $LaBr_3$ detectors and a rotating disk with a 30 cm diameter. Rotation of the disk with a stepping motor allowed to change the set of three targets between the detector pairs. The rotating disk had 16 places for samples. Depending on the number of targets, an adequate rotating sequence was applied. The sequence was optimized so that the initial activity of all irradiated targets was measured after a minimal number of rotations.

After the irradiation, the targets were placed on the disk. In the case of irradiation of 15 targets with 58 MeV beam energy, the disk was following a pre-planned sequence of rotations, so that the activity of each target could be measured. Time intervals depended on the sequence, which was planned so that they were short in the beginning (less than 10 s) and got gradually longer, up to 900 s. After the irradiation of three targets with 40 MeV beam energy, their activity was measured continuously by the three detector pairs, without any rotation. In this case, the time intervals were later set according to the number of registered counts.

Table 2 Details of irradiations

Number of targets	Energy [MeV]	Flux [$cm^{-2}\cdot s^{-1}$]	Irradiation time [s]
15	58	$1.88\cdot10^8$	154.5
3	40	$1.59\cdot10^8$	140.5

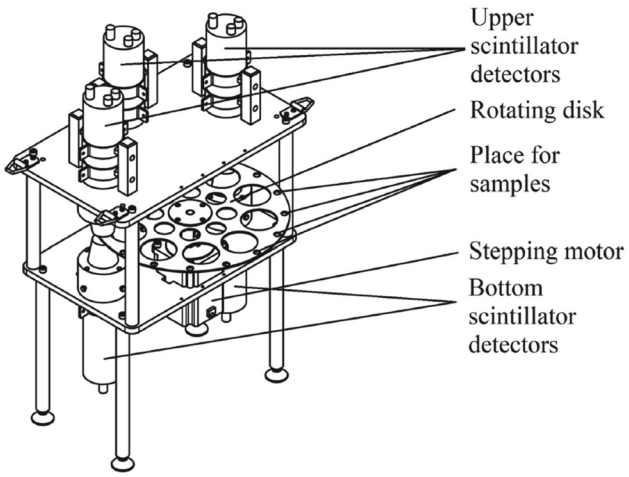

Fig. 1 Detection setup

The scintillation detectors were arranged in a triggerless mode using a CAEN DT5730SB digitizer, with a sampling rate of 500 MHz. The rotating disk was controlled by a 1.8° stepper motor (model 85BYGH450B). The control signals of the stepper motor were recorded, also from the digitizer, to synchronize the measurement with the rotations of the disk. The detectors were coupled with three 1-inch $LaBr_3$ crystals (Philips XP2972 PMTs) on the top side and three 1.5-inch $LaBr_3$ crystals (EMI 9814B PMTs) on the bottom. The CAEN DT5730SB digitizer was selected since it could handle up to 8 channels, thus allowing simultaneous acquisition for all detectors. It first optimizes the spectrum mode for the best parameters: input voltage (peak-to-peak), threshold, charge sensitivity, signal integration time, and background suppression. Then, it switched to list mode for fast signal processing. In the list mode, every recorded signal was saved with its timestamp (precision of 2 ns) for later use in offline coincidence analysis. The coincidence window was set at 30 ns, allowing the recording of pairs of 511 keV γ-quanta from opposite detectors. As the measurements of activity started approximately 5 min after the irradiation, random coincidences were found negligible. This was verified by monitoring the coincidences between detectors not belonging to a pair. The number of coincidence counts in the top-bottom detector pairs was at least three orders of magnitude higher than for other detector pairs. This observation agrees with the conclusions of Horst et al. [6], where the coincidence rate between the $LaBr_3$ module placed perpendicular to the pair of detectors effectively vanished after 2 min. High voltage to the photomultiplier tubes was delivered through a LeCroy HV4032A-32-channel power supply with a precision of ± 1 V. This provided a very stable measurement environment, while the rotational sequence of the disk was optimized with respect to the trade-off between initial activity measurement and sufficient statistical accuracy during the decay process.

3 Data analysis

Since the targets were close to each other during measurement, the activity obtained from single spectra included also the activity of neighbouring targets. For this reason, the experimental results presented in this paper are based on coincidence detection of two 511 keV photons following e^+e^- annihilation after β^+ decay. Detector efficiency was determined after a measurement of ^{22}Na source with known activity. The three detector pairs had efficiency of 1.692(5)%, 1.820(6)% and 1.896(6)% in the coincidence measurement. The energies at which each target was irradiated were obtained using the Bethe-Bloch formula, and they were calculated at the center of the targets.

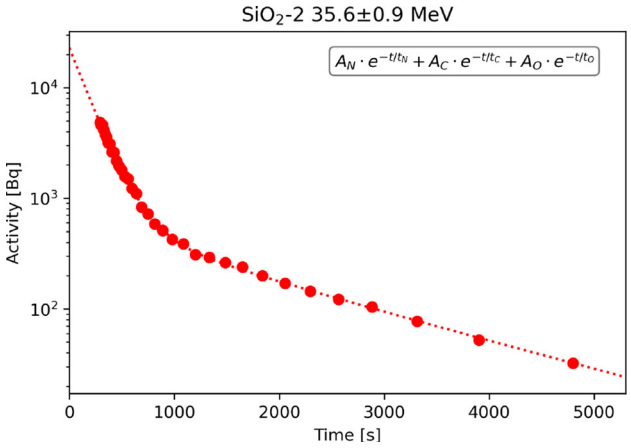

Fig. 2 Example of a decay curve. Dotted line is the fit of function (1) to the measured activity marked with red dots

Activity of an irradiated target decreases with time according to a formula that is a sum of exponential functions:

$$A(t) = \sum_{i=C,N,O} A_i \cdot e^{-t/t_i}, \tag{1}$$

where t is time, A_i is the activity of isotope i at the end of the irradiation, and t_i is its lifetime. The indexes C, N and O correspond to produced isotopes listed in Table 1: ^{11}C, ^{13}N and ^{15}O respectively. Function (1) was fitted to experimental data to obtain the activities A_i. An example of a decay curve with the fitted function is presented on Fig. 2. In the beginning, the activity comes mostly from ^{15}O, which has the shortest lifetime, and in the end it comes almost only from ^{11}C decay.

The lowest energy at which a target was irradiated was 12 ± 2 MeV, which is much lower than the Q-value for reaction ^{16}O(p,d+α)^{11}C, equal to 23.7 MeV. Therefore, in this case the fitted function did not include the activity of ^{11}C:

$$A(t) = \sum_{i=N,O} A_i \cdot e^{-t/t_i}. \tag{2}$$

Activities at the end of the irradiation A_i were used to determine the cross section σ_i of the reaction in which isotope i is produced, according to the formula

$$\sigma_i = \frac{A_i}{N_T \cdot I \cdot (1 - e^{-\lambda_i t_{EOB}})}, \tag{3}$$

where N_T is the number of oxygen nuclei in a target, I is the beam flux, λ_i is the decay constant of isotope i and t_{EOB} is the time of irradiation ("end of beam" time). N_T was determined from mass measurement of the targets. The uncertainty of the cross section takes into consideration only the uncertainty of A_i obtained from the fit. The systematic error is estimated at 1%, with the largest contribution coming from the uncertainty of the beam flux. The proton beam flux I for subsequent targets is reduced compared to the initial one, due to the

inelastic processes. This effect (∼3% after 10 targets) was taken into account through absorption calculations based on total inelastic cross sections [12].

4 Results and Discussion

The results are presented on Fig. 3 and in Table 3. For comparison, selected data from literature is also plotted. Results from this work were compared to measurements by Masuda et al. [5], Akagi et al. [4], Horst et al. [6] and Rodríguez-González et al. [7], which are the most recent available data at this energy range.

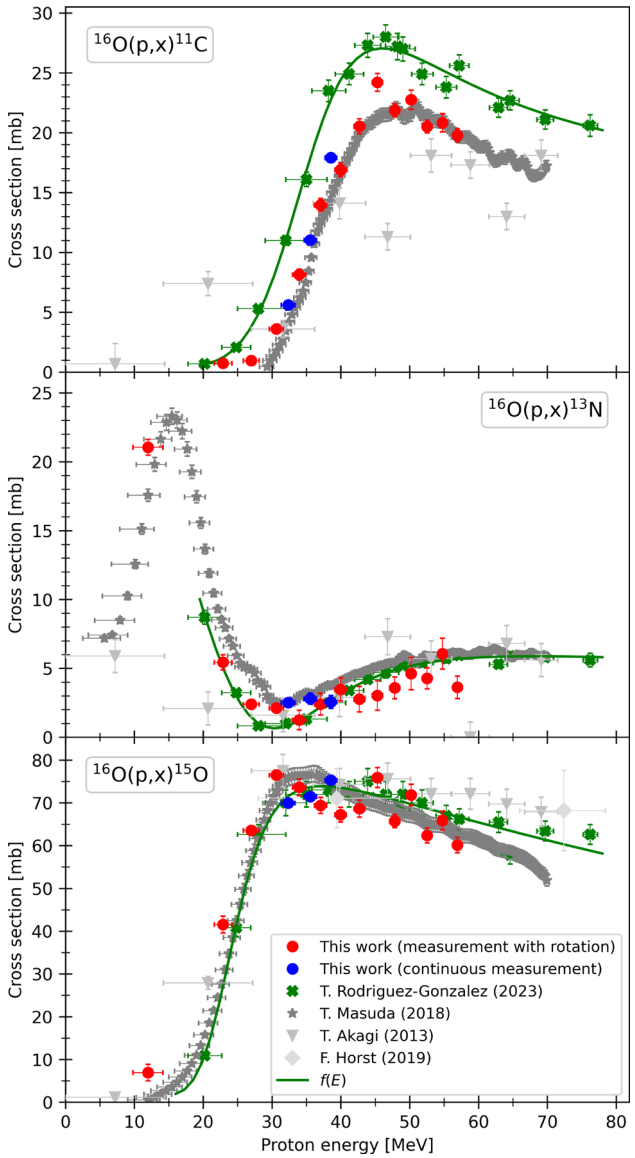

Fig. 3 Cross section of reactions ^{16}O(p,x)^{11}C, ^{16}O(p,x)^{13}N and ^{16}O(p,x)^{15}O in the function of proton energy. Results from this work are marked in red and blue points. Grey and green marks correspond to data from literature

Table 3 Cross section of reactions ^{16}O(p,x)^{11}C, ^{16}O(p,x)^{13}N and ^{16}O(p,x)^{15}O

Energy [MeV]	$\sigma(^{11}\mathrm{C})$ [mb]	$\sigma(^{13}\mathrm{N})$ [mb]	$\sigma(^{15}\mathrm{O})$ [mb]
56.9 ± 0.6	19.8 ± 0.6	3.6 ± 0.8	60.1 ± 1.8
54.8 ± 0.6	20.8 ± 0.8	6.1 ± 1.1	65.9 ± 2.2
52.5 ± 0.7	20.5 ± 0.5	4.3 ± 0.8	62.4 ± 1.7
50.2 ± 0.7	22.8 ± 0.8	4.6 ± 1.2	71.8 ± 2.5
47.8 ± 0.7	21.9 ± 0.5	3.6 ± 0.8	65.7 ± 1.5
45.3 ± 0.8	24.2 ± 0.7	3.0 ± 1.1	75.9 ± 2.3
42.7 ± 0.8	20.5 ± 0.6	2.8 ± 0.9	68.6 ± 2.0
40.0 ± 0.8	16.9 ± 0.6	3.5 ± 0.8	67.2 ± 1.7
38.6 ± 0.8	*17.9 ± 0.3*	*2.6 ± 0.5*	*75.3 ± 1.0*
37.0 ± 0.9	14.0 ± 0.5	2.4 ± 0.8	69.4 ± 1.9
35.6 ± 0.9	*11.0 ± 0.3*	*2.8 ± 0.4*	*71.5 ± 0.9*
33.9 ± 0.9	8.2 ± 0.5	1.2 ± 0.7	73.6 ± 1.9
32.3 ± 1.0	*5.6 ± 0.2*	*2.5 ± 0.2*	*70.0 ± 0.6*
30.6 ± 1.0	3.6 ± 0.2	2.1 ± 0.3	76.5 ± 1.2
27.0 ± 1.1	1.0 ± 0.1	2.4 ± 0.2	63.5 ± 0.9
22.9 ± 1.3	0.7 ± 0.3	5.4 ± 0.5	41.5 ± 2.0
12.0 ± 2.2	–	21.0 ± 0.6	6.9 ± 1.9

Results obtained in a measurement without rotation in the detection setup are shown in italics

As the threshold for the ^{16}O(p,α)^{13}N is the lowest, the cross section for this reaction rises first with increasing proton energy, reaching a maximum around $E_p \simeq 15$ MeV. The excitation function falls down to a minimum at ∼30 MeV, slowly rising afterwards. The production cross section of ^{15}O and ^{11}C have similar shape, displaced in energy due to the different threshold (see Table 1).

The observed energy dependence of measured cross section is similar to the results by Masuda et al. for all three reactions. Few results of the measurements by Akagi et al. seem to be out of this trend, particularly at ∼47 MeV in the case of ^{11}C production. We observe also a good agreement of our data with the measurements of Rodríguez-González et al. except the reaction leading to the production of ^{11}C. The experimental data of Rodríguez-González were fitted [13] for six reactions by a general formula $f(E)$ - ratio of 4$^{\text{th}}$ to 5$^{\text{th}}$ order polynomials, 10 free parameters per reaction. (Please note the values of the parameters in the Table IX of that paper are printed in reversed order, i.e. value of a_4 corresponds to a_0.) We evaluate the agreement of our results to this parametrization $f(E)$. The following criteria were used: (i) χ^2 value defined as $\sum \frac{(\sigma_i - f(E_i))^2}{\Delta\sigma_i^2}$, (ii) ratio of experimental cross section to the parametrization function $r = \frac{\sigma_i}{f(E_i)}$, (iii) pull, defined as $p = \frac{1}{N} \sum \frac{\sigma_i - f(E_i)}{\Delta\sigma_i}$ and (iv) A-factor defined as $A = \frac{1}{N} \Sigma \frac{|\sigma_i - f(E_i)|}{\sigma_i + f(E_i)}$. Here σ_i denotes the experimental

Table 4 Parameters describing the agreement of experimental cross section on ^{16}O with the analytical function [13]

Residue	χ^2/N	r	p	A-factor
^{15}O	19	1.03 ± 0.16	0.5 ± 4.4	0.05
^{13}N	4.5	1.1 ± 0.7	0.2 ± 2.1	0.14
^{11}C	180	0.69 ± 0.18	-11 ± 7	0.20

See text for details

cross section with the uncertainty $\Delta\sigma_i$, measured at the proton energy E_i and N is the number of experimental results. It should be noted, that the uncertainty of the function $f(E)$ is not specified, so the χ^2 values should not be treated according to their standard statistical interpretation. The value of the pull variable p shows the systematical deviation of experimental results with respect to the function $f(E)$ in units of experimental uncertainties (low value shows the results are scattered above and below the function). The A-factor [14] indicates the strength of the relative difference (0 for perfect agreement and 1 in the opposite case). The evaluated parameters, provided in Table 4, clearly indicate that the results of actual measurements are in relatively good agreement in the cases of ^{16}O(p,d)^{15}O and ^{16}O(p,α)^{13}N reactions, while they are systematically 30% below in the case of ^{16}O(p,d+α)^{11}C reaction.

5 Conclusion

Cross sections for reactions on oxygen leading to the production of β^+ emitting nuclei ^{11}C, ^{13}N and ^{15}O were obtained for proton energies below 60 MeV. The beam was provided by the AIC-144 cyclotron of the Institute of Nuclear Physics in Kraków. Silicon dioxide was used as the target. The proton-induced reactions on silicon had minimal influence on the measurements as the produced nuclei have much shorter lifetimes compared to ^{11}C, ^{13}N and ^{15}O.

These findings contribute to a deeper understanding of the significance of nuclear reactions in proton therapy. The results of the experiment agree (with a few local exceptions) with several previous measurements, including the one using Cherenkov radiation in bulk SiO_2 [5]. Our results for the ^{16}O(p,d+α)^{11}C reaction are 30% below that reported in recent extensive measurements [13], while compatible results were obtained for other reaction channels.

The application of classical nuclear physics techniques, as employed in this study, validates the results obtained in previous experiments. However, the systematic difference observed in the case of ^{16}O(p,x)^{11}C with respect to the recent results of Rodríguez-González et al., highlights the need for a reexamination of this reaction, not only at the same energy but also with protons accelerated to higher energies. Additional verification is needed, as this cross section contributes to dose evaluation for patients undergoing proton therapy.

Data Availability Statement My manuscript has no associated data. [Author's comment: Data sharing not applicable to this article as all generated data are included in the paper.]

Code Availability Statement My manuscript has no associated code/software. [Author's comment: Code/Software sharing not applicable to this article as all equations used in the calculations are included in the paper.]

Appendix

This appendix provides several experimental details (see Table 5) concerning proton-oxygen interactions, leading to the production of β^+ emitters, that have been studied in the past six decades. The reactions were intensively measured half a century ago (see Fig. 4), while later the experiments were quite rare in spite of the technological progress in instrumentation. The experiments selected for this comparison can be grouped into several (non-exclusive) categories:

- low-energy studies of the total cross section, inspired by the astrophysical importance of proton burning on oxygen,
- low-energy studies of angular distribution of elastic (p,p) and inelastic (for example (p,α)) scattering needed for the evaluation of various aspects of optical models,
- low-energy-studies around the Bragg peak for the possible measurement of the distal fall-off of the proton range distribution in proton beam therapy,
- measurements at intermediate energies (few tens MeV to few hundred MeV) for the general knowledge on the proton inelastic processes influencing flux reduction in proton beam therapy, and
- measurements at relativistic energies $T \geq m_p c^2$, where the cross section is not expected to show significant energy dependence [15], while the experimental values are important for various applications of nuclear spallation by protons (e.g. accelerator-driven system, neutrino beam etc.).

Table 5 Details of selected experiments studying proton+oxygen interactions

Year	Energy	Target	Method	Detector	References
1958	6–14.5 MeV	Gelva $C_4H_6O_2$	511 keV activity	NaI	[17]
1960	5.7 GeV	Anhydrous oxalic acid	511 keV activity	$1 \times 1\frac{1}{2}$ NaI(Tl)	[18]
1960	362 ± 15 MeV	Sistilled water, LiOH	511 keV activity	G–M counter	[19,20]
1960	9.7–15 MeV	$Na_2B_4O_7 \cdot 2H_2O$	$e^+e^- \rightarrow \gamma\gamma$ coincidence	NaI(Tl) 1.5 in × 1 in	[21]
1961	12–18 MeV	Mylar	Activity after 5 min	G–M counter	[22]
1961	13.5–18.1 MeV	O_2 gas, CH_2 foil, C_3H_8	Charged particles	Ionization chamber	[23]
1962	20–150 MeV	Sintered BeO	511 keV activity	Scintillation detector	[24]
1962	146 ± 7 MeV	Water	511 keV activity	NaI(Tl) 5 cm × 5 cm	[25]
1964	4.2–8.6 MeV	O_2 gas	Charged particles	CsI(Tl)	[26]
1965	30–155 MeV 5.7 GeV	Sintered BeO	511 keV activity	NaI(Tl) of different sizes	[27]
1967	13.1(7) MeV	Gas active target	Charged particles	Cloud chamber (triggered)	[28]
1969	38 MeV	Mylar	Charged particles	Si counter (1.8 mm)	[29]
1971	50, 100, 153 MeV	SiO_2, H_2O	511 keV activity	NaI(Tl), Ge(Li)	[30]
1973	6.5–7.7 MeV	MgO_2	511 keV activity	NaI(Tl) 7.6 cm × 7.6 cm	[31]
1973	5.4–9.9 MeV	WO_3	$e^+e^- \rightarrow \gamma\gamma$ coincidence	Pair of NaI(Tl) 7.6 cm × 7.6 cm	[32]
1977	6.7–9.2 MeV	O_2 gas 0.3–0.4 bar	$e^+e^- \rightarrow \gamma\gamma$ coincidence	Pair of NaI(Tl) 7.6 cm × 7.6 cm	[33]
1986	6.5–16.5 MeV	O_2 gas +2% NO_2	511 keV activity	NaI(Tl)	[34]
1989	5–30 MeV	O_2 gas 10 bar	$e^+e^- \rightarrow \gamma\gamma$ coincidence	Pair of NE102 scintillators	[35]
2013	14–70 MeV	Gelatinous water	$e^+e^- \rightarrow \gamma\gamma$ coincidence	PET scanner	[4]
2018	5–70 MeV	Bulk SiO_2	Cherenkov radiation of β^+	Electron-multiplying CCD	[5]
2019	40–220 MeV	BeO	$e^+e^- \rightarrow \gamma\gamma$ coincidence	3 BaF_2 3.5 × 3.5 × 7 cm^3	[6]
2022	3–18 MeV	PMMA Nylon-6	$e^+e^- \rightarrow \gamma\gamma$ coincidence	PET scanner	[13]
2022	3–6 MeV	He gas (inv. kinematics)	Charged particles	MUSIC	[16]
2023	20–200 MeV	SiO_2	$e^+e^- \rightarrow \gamma\gamma$ coincidence	PET scanner	[7]

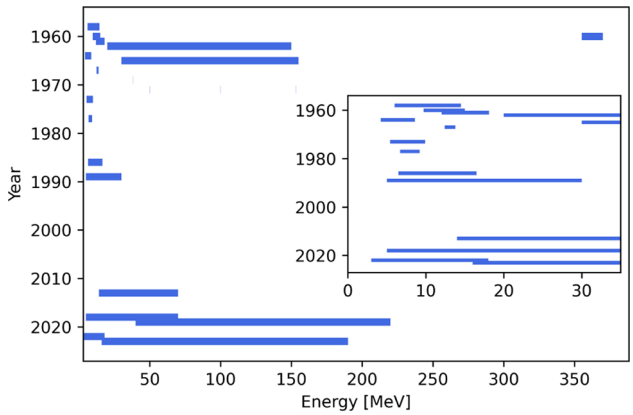

Fig. 4 Range of proton energies used in p+^{16}O measurements and the year of publication of the result, as listed in the Table 5

The production of β^+ emitters was studied through the annihilation process $e^+e^- \rightarrow \gamma\gamma$. Initially, only one of the 511 keV photons was detected, predominantly in a NaI(Tl) spectrometer. Later, a setup composed of a pair of detectors allowed for coincident measurement of both 511 keV photons. The use of PET scanners belongs to this category. Random coincidences were found to be insignificant 2 min after the irradiation, what was carefully checked using the coincidences of the third BaF_2 detector compared to the pair of modules placed back-to-back [6]. In all cases, the time-resolved decay of the produced activity allows to identify reaction channels with quite different half-lives. A novel method was the measurement of the Cherenkov light emitted by the positron in the β^+ decay of radionuclides produced in SiO_2 bulk crystal irradiated with proton beam [5]. The Cherenkov light intensity was then normalized to a selected experimental value. In order not to be influenced by short-lived activities produced on Si isotopes, the measurement started 2 min after the end of beam. This delay is shorter compared to the typical time of 5–20 min needed to move the irradiated target from the beam zone to the measuring station. One should mention here the recent study of the reaction $^{13}N + \alpha \rightarrow {}^{16}O+p$ in inverse kinematics with exotic ^{13}N beam [16].

The use of the oxygen gas target was rather limited to the angular distribution measurements. Numerous compounds rich in oxygen were used as targets. Water is an interesting option, as at energies below the pion production threshold (∼280 MeV) proton-proton interactions are elastic only.

Unfortunately, thin and portable water target, needed for off-beam decay spectroscopy, is rather not feasible. The solid compounds, like the already mentioned SiO_2, should contribute to the β^+ yield only by short half-life isotopes.

References

1. W.D. Newhauser, R. Zhang, The physics of proton therapy. Phys. Med. Biol. **60**(8), R155 (2015)
2. V. Conte, S. Agosteo, A. Bianchi, D. Bolst, D. Bortot, R. Catalano, G.A.P. Cirrone, P. Colautti, G. Cuttone, S. Guatelli et al., Microdosimetry of a therapeutic proton beam with a mini-TEPC and a MicroPlus-Bridge detector for RBE assessment. Phys. Med. Biol. **65**(24), 245018 (2020)
3. F. Tommasino, M. Durante, Proton radiobiology. Cancers **7**(1), 353–381 (2015)
4. T. Akagi, M. Yagi, T. Yamashita, M. Murakami, Y. Yamakawa, K. Kitamura, K. Ogura, K. Kondo, S. Kawanishi, Experimental study for the production cross sections of positron emitters induced from ^{12}C and ^{16}O nuclei by low-energy proton beams. Radiat. Meas. **59**, 262–269 (2013)
5. T. Masuda, J. Kataoka, M. Arimoto, M. Takabe, T. Nishio, K. Matsushita, T. Miyake, S. Yamamoto, T. Inaniwa, T. Toshito, Measurement of nuclear reaction cross sections by using Cherenkov radiation toward high-precision proton therapy. Sci. Rep. **8**(1), 2570 (2018)
6. F. Horst, W. Adi, G. Aricò, K.-T. Brinkmann, M. Durante, C.-A. Reidel, M. Rovituso, U. Weber, H.-G. Zaunick, K. Zink et al., Measurement of PET isotope production cross sections for protons and carbon ions on carbon and oxygen targets for applications in particle therapy range verification. Phys. Med. Biol. **64**(20), 205012 (2019)
7. T. Rodríguez-González, C. Guerrero, C.M. Bäcker, J. Bauer, C. B.äumer, S. Brons, W. Jentzen, M.C. Jiménez-Ramos, M. de los Ángeles Millán-Callado, C. Schömers, et al., Production of ^{11}C, ^{13}N and ^{15}O in proton-induced nuclear reactions up to 200 MeV. Nucl. Data Sheets **187**, 579–596 (2023)
8. I. Skwira-Chalot, P. Sękowski, J. Matulewicz, S. Kusyk, A. Spyra, J. Swakoń, W. Szcześniak, A. Taranienko, D. Wróbel, T. Matulewicz, SiO_2 as oxygen target to study nuclear reactions induced by protons in the hadrontherapy energy range. AIP Conf. Proc. **3054**, 040006 (2024)
9. NNDC Database NuDat 3.0. https://www.nndc.bnl.gov/nudat3/
10. JANIS Web. https://www.oecd-nea.org/janisweb/
11. P. Sękowski, G. Saworska, I. Skwira-Chalot, A. Spyra, W. Szcześniak, T. Matulewicz, T. Horwacik, J. Swakoń, Reconstruction of gamma-ray source activity in a multiple samples set-up. Nuclear Inst. Methods Phys. Res. A **1040**, 167292 (2022)
12. M. Enferadi, S. Sarbazvatan, M. Sadeghi, J.-H. Hong, C.-J. Tung, T.-C. Chao, C.-C. Lee, S.-P. Wey, Nuclear reaction cross sections for proton therapy applications. J. Radioanal. Nucl. Chem. **314**, 1207–1235 (2017)
13. T. Rodríguez-González, C. Guerrero, M. del Carmen Jiménez-Ramos, J. Lerendegui-Marco, M. de los Ángeles Millán-Callado, Á. Parrado, J. Gómez, J.M. Quesada. Production yields at the distal fall-off of the β+ emitters ^{11}C and ^{13}N for in-vivo range verification in proton therapy. Radiat. Phys. Chem. **190**, 109759 (2022)
14. S.K. Sharma, B. Kamys, F. Goldenbaum, D. Filges, Ranking and validation of spallation models for isotopic production cross sections of heavy residua. Eur. Phys. J. A **53**, 1–7 (2017)
15. N.A. McCubbin, Proton-nucleus dynamics at ultra-relativistic energies. Nucl. Phys. A **488**, 585–598 (1988)
16. H. Jayatissa, M.L. Avila, K.E. Rehm, R. Talwar, P. Mohr, K. Auranen, J. Chen, D.A. Gorelov, C.R. Hoffman, C.L. Jiang et al., First direct measurement of the ^{13}N(α, p)^{16}O reaction relevant for core-collapse supernovae nucleosynthesis. Phys. Rev. C **105**(4), L042802 (2022)
17. A.B. Whitehead, J.S. Foster, Activation cross sections for C^{12}(p, pn)C^{11}, O^{16}(p,α)N^{13}, and F^{19}(p, pn)F^{18}. Can. J. Phys. **36**(10), 1276–1285 (1958)

18. P.A. Benioff, Nuclear reactions of low-Z elements with 5.7-BeV protons. Phys. Rev. **119**(1), 316 (1960)
19. V. Parikh, The activities induced in beryllium, oxygen and fluorine by protons of 220 MeV to 362 MeV. Nucl. Phys. **18**, 646–653 (1960)
20. V. Parikh, Absolute cross-sections of C^{12}(p, pn)C^{11} from 288 to 383 MeV. Nucl. Phys. **18**, 628–637 (1960)
21. M. Furukawa, Y. Ishizaki, Y. Nakano, T. Nozaki, Y. Saji, S. Tanaka, Excitation function for the reaction B^{11}(p, n)C^{11} up to E_p=15 MeV and energy levels of C^{12}. J. Phys. Soc. Jpn. **15**(12), 2167–2170 (1960)
22. H.A. Hill, E.L. Haase, D.B. Knudsen, High-resolution measurements of the O^{16}(p, α)N^{13} excitation function. Phys. Rev. **123**(4), 1301 (1961)
23. D.R. Maxson, O^{16}(p,α)N^{13} angular distributions at 13.5–18.1 MeV. Phys. Rev. **123**(4), 1304 (1961)
24. G. Albouy, J.-P. Cohen, M. Gusakow, N. Poffe, H. Sergolle, L. Valentin, Spallation de l'oxygene par les protons de 20 a 150 MeV. Phys. Lett. **2**, 306 (1962)
25. K.J. Foley, G.L. Salmon, A.B. Clegg, Gamma radiation from the bombardment of ^{16}O and ^{19}F nuclei with 150 MeV protons. Nucl. Phys. **31**, 43–52 (1962)
26. R.L. Dangle, L.D. Oppliger, G. Hardie, O^{16}(p,α)N^{13} and O^{16}(p, p')O^{16*} differential cross sections. Phys. Rev. **133**(3B), B647 (1964)
27. L. Valentin, Réactions (p, n) et (p, pn) induites à moyenne énergie sur des noyaux légers. Nucl. Phys. **62**(1), 81–102 (1965)
28. R. Chapman, A.M. MacLeod, Proton nuclear reaction cross sections in oxygen and neon at 13 MeV. Nucl. Phys. A **94**(2), 313–323 (1967)
29. G. Gambarini, I. Iori, S. Micheletti, N. Molho, M. Pignanelli, G. Tagliaferri, Study of (p,α) reactions in light nuclei at 38 MeV. Nucl. Phys. A **126**(3), 562–576 (1969)
30. R. Bimbot, H. Gauvin, Réactions de spallation de noyaux légers induites par des protons de 50, 100 et 153 MeV. Compte. Rendu. **273**, 1054 (1971)
31. R.H. McCamis, G.A. Moss, J.M. Cameron, Total cross section of ^{16}O(p,α)^{13}N from threshold to . Can. J. Phys. **51**(16), 1689–1692 (1973)
32. A.V. Nero, A.J. Howard, ^{16}O(p,α_0)^{13}N cross-section measurements. Nucl. Phys. A **210**(1), 60–66 (1973)
33. W. Gruhle, B. Kober, The reactions ^{16}O(p,α), ^{20}Ne(p,α) and ^{24}Mg(p,α). Nucl. Phys. A **286**(3), 523–530 (1977)
34. M. Sajjad, R.M. Lambrecht, A.P. Wolf, Cyclotron isotopes and radiopharmaceuticals. XXXVII. Excitation functions for the ^{16}O(p,α)^{13}N and ^{14}N(p,pn)^{13}N reactions. Radiochim. Acta **39**(3), 165–168 (1986)
35. S.W. Kitwanga, P. Leleux, P. Lipnik, J. Vanhorenbeeck, Production of ^{13}N radioactive nuclei from ^{13}C(p, n) or ^{16}O(p,α) reactions. Phys. Rev. C **40**(1), 35 (1989)